ACTION GUIDANCE: GETTING THE BEST OF SPARSE REWARDS AND SHAPED REWARDS FOR REAL-TIME STRATEGY GAMES

Shengyi Huang
College of Computing & Informatics
Drexel University
Philadelphia, PA 19104
sh3397@drexel.edu

Santiago Ontañón *
College of Computing & Informatics
Drexel University
Philadelphia, PA 19104
so367@drexel.edu

ABSTRACT

Training agents using Reinforcement Learning in games with sparse rewards is a challenging problem, since large amounts of exploration are required to retrieve even the first reward. To tackle this problem, a common approach is to use reward shaping to help exploration. However, an important drawback of reward shaping is that agents sometimes learn to optimize the shaped reward instead of the true objective. In this paper, we present a novel technique that we call *action guidance* that successfully trains agents to eventually optimize the true objective in games with sparse rewards while maintaining most of the sample efficiency that comes with reward shaping. We evaluate our approach in a simplified real-time strategy (RTS) game simulator called μRTS.

Training agents using Reinforcement Learning with sparse rewards is often difficult (Pathak et al., 2017). First, due to the sparsity of the reward, the agent often spends the majority of the training time doing inefficient exploration and sometimes not even reaching the first sparse reward during the entirety of its training. Second, even if the agents have successfully retrieved some sparse rewards, performing proper credit assignment is challenging among complex sequences of actions that have led to theses sparse rewards. Reward shaping (Ng et al., 1999) is a widely-used technique designed to mitigate this problem. It works by providing intermediate rewards that lead the agent towards the sparse rewards, which are the true objective. For example, the sparse reward for a game of Chess is naturally +1 for winning, -1 for losing, and 0 for drawing, while a possible shaped reward might be +1 for every enemy piece the agent takes. One of the critical drawbacks for reward shaping is that the agent sometimes learns to optimize for the shaped reward instead of the real objective. Using the Chess example, the agent might learn to take as many enemy pieces as possible while still losing the game. A good shaped reward achieves a nice balance between letting the agent find the sparse reward and being too shaped (so the agent learns to just maximize the shaped reward), but this balance can be difficult to find.

In this paper, we present a novel technique called *action guidance* that successfully trains the agent to eventually optimize over sparse rewards while maintaining most of the sample efficiency that comes with reward shaping. It works by constructing a *main agent* that only learns from the sparse reward function $R_{\mathcal{M}}$ and some *auxiliary agents* that learn from the shaped reward function $R_{\mathcal{A}_1}, R_{\mathcal{A}_2}, \ldots, R_{\mathcal{A}_n}$. During training, we use the same rollouts to train the main and auxiliary agents and initially set a high-probability of the main agent to take *action guidance* from the auxiliary agents, that is, *the main agent will execute actions sampled from the auxiliary agents*. Then the main agent and auxiliary agents are updated via off-policy policy gradient. As the training goes on, the main agent will get more independent and execute more actions sampled from its own policy. Auxiliary agents learn from shaped rewards and therefore make the training sample-efficient, while the main agent learns from the original sparse reward and therefore makes sure that the agents will eventually optimize over the true objective. We can see action guidance as combining reward shaping to train auxiliary agents interlieaved with a sort of imitation learning to guide the main agent from these auxiliary agents.

---

*Currently at Google

1

We examine action guidance in the context of a real-time strategy (RTS) game simulator called μRTS for three sparse rewards tasks of varying difficulty. For each task, we compare the performance of training agents with the sparse reward function $R_{\mathcal{M}}$, a shaped reward function $R_{\mathcal{A}_1}$, and action guidance with a singular auxiliary agent learning from $R_{\mathcal{A}_1}$. The main highlights are:

Action guidance is sample-efficient. Since the auxiliary agent learns from $R_{\mathcal{A}_1}$ and the main agent takes action guidance from the auxiliary agent during the initial stage of training, the main agent is more likely to discover the first sparse reward more quickly and learn more efficiently. Empirically, action guidance reaches almost the same level of sample efficiency as reward shaping in all of the three tasks tested.

The true objective is being optimized. During the course of training, the main agent has never seen the shaped rewards. This ensures that the main agent, which is the agent we are really interested in, is always optimizing against the true objective and is less biased by the shaped rewards. As an example, Figure 1 shows that the main agent trained with action guidance eventually learns to win the game as fast as possible, even though it has only learned from the match outcome reward (+1 for winning, -1 for losing, and 0 for drawing). In contrast, the agents trained with reward shaping learn more diverse sets of behaviors which result in high shaped reward.

To support further research in this field, we make our source code available at GitHub[1], as well as all the metrics, logs, and recorded videos[2].

1 RELATED WORK

In this section, we briefly summarize the popular techniques proposed to address the challenge of sparse rewards.

Reward Shaping. Reward shaping is a common technique where the human designer uses domain knowledge to define additional intermediate rewards for the agents. Ng et al. (1999) show that a slightly more restricted form of state-based reward shaping has better theoretical properties for preserving the optimal policy.

Transfer and Curriculum Learning. Sometimes learning the target tasks with sparse rewards is too challenging, and it is more preferable to learn some easier tasks first. *Transfer learning* leverages this idea and trains agents with some easier source tasks and then later transfer the knowledge through value function (Taylor et al., 2007) or reward shaping (Svetlik et al., 2017). *Curriculum learning* further extends transfer learning by automatically designing and choosing a full sequences of source tasks (i.e. a curriculum) (Narvekar & Stone, 2018).

Imitation Learning. Alternatively, it is possible to directly provide examples of human demonstration or expert replay for the agents to mimic via Behavior Cloning (BC) (Bain & Sammut, 1995), which uses supervised learning to learn a policy given the state-action pairs from expert replays. Alternatively, Inverse Reinforcement Learning (IRL) (Abbeel & Ng, 2004) recovers a reward function from expert demonstrations to be used to train agents.

Curiosity-driven Learning. Curiosity driven learning seeks to design *intrinsic* reward functions (Burda et al., 2019) using metrics such as prediction errors (Houthooft et al., 2016) and "visit counts" (Bellemare et al., 2016; Lopes et al., 2012). These intrinsic rewards encourage the agents to explore unseen states.

Goal-oriented Learning. In certain tasks, it is possible to describe a goal state and use it in conjunction with the current state as input (Schaul et al., 2015). Hindsight experience replay (HER) (Andrychowicz et al., 2017) develops better utilization of existing data in experience replay by replaying each episode with different goals. HER is shown to be an effective technique in sparse rewards tasks.

Hierarchical Reinforcement Learning (HRL). If the target task is difficult to learn directly, it is also possible to hierarchically structure the task using experts' knowledge and train hierarchical

---

[1] `https://github.com/anonymous-research-code/action-guidance`
[2] `https://app.wandb.ai/vwxyzjn/action-guidance`

(a) shaped reward
(https://streamable.com/o797ca)

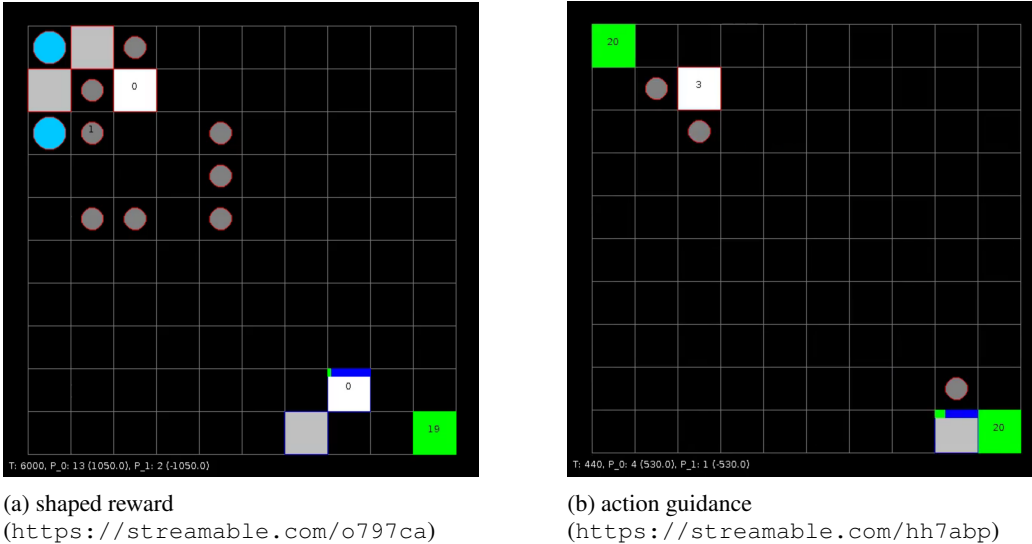(b) action guidance
(https://streamable.com/hh7abp)

Figure 1: The screenshot shows the typical learned behavior of agents in the task of DefeatRandomEnemy. (a) shows that an agent trained with some shaped reward function $R_{\mathcal{A}_1}$ learns many helpful behaviors such as building workers (grey circles), combat units (blue circles), and barracks (grey square) or using owned units (with red boarder) to attack enemy units (with blue border), but does not learn to win as fast as possible (i.e. it still does not win at internal time step $t = 6000$). In contrast, (b) shows an agent trained with action guidance optimizes over the match outcome and learns to win as fast as possible (i.e. about to win the game at $t = 440$), with its main agent learning from the match outcome reward function $R_{\mathcal{M}}$ and a singular auxiliary agent learning from the same shaped reward function $R_{\mathcal{A}_1}$. Click on the link below figures to see the full videos of trained agents.

agents, which generally involves a main agent that learns abstract goals, time, and actions, as well as auxiliary agents that learn primitive actions and specific goals (Dietterich, 2000). HRL is especially popular in RTS games with combinatorial action spaces (Pang et al., 2019; Ye et al., 2020).

The most closely related work is perhaps Scheduled Auxiliary Control (SAC-X) (Riedmiller et al., 2018), which is an HRL algorithm that trains auxiliary agents to perform primitive actions with shaped rewards and a main agent to schedule the use of auxiliary agents with sparse rewards. However, our approach differs in the treatment of the main agent. Instead of learning to *schedule* auxiliary agents, our main agent learns to act in the entire action space by *taking action guidance* from the auxiliary agents. There are two intuitive benefits to our approach since our main agent learns in the full action space. First, during policy evaluation our main agent does not have to commit to a particular auxiliary agent to perform actions for a fixed number of time steps like it is usually done in SAC-X. Second, learning in the full action space means the main agent will less likely suffer from the definition of hand-crafted sub-tasks, which could be incomplete or biased.

2 BACKGROUND

We consider the Reinforcement Learning problem in a Markov Decision Process (MDP) denoted as $(S, A, P, \rho_0, r, \gamma, T)$, where S is the state space, A is the discrete action space, $P : S \times A \times S \to [0, 1]$ is the state transition probability, $\rho_0 : S \to [0, 1]$ is the the initial state distribution, $r : S \times A \to \mathbb{R}$ is the reward function, γ is the discount factor, and T is the maximum episode length. A stochastic policy $\pi_\theta : S \times A \to [0, 1]$, parameterized by a parameter vector θ, assigns a probability value to an action given a state. The goal is to maximize the expected discounted return of the policy:

$$\mathbb{E}_\tau \left[\sum_{t=0}^{T-1} \gamma^t r_t \right], \quad \text{where } \tau \text{ is the trajectory } (s_0, a_0, r_0, s_1, \ldots, s_{T-1}, a_{T-1}, r_{T-1})$$
$$\text{and } s_0 \sim \rho_0, s_t \sim P(\cdot | s_{t-1}, a_{t-1}), a_t \sim \pi_\theta(\cdot | s_t), r_t = r(s_t, a_t)$$

3

Policy Gradient Algorithms. The core idea behind policy gradient algorithms is to obtain the *policy gradient* $\nabla_\theta J$ of the expected discounted return with respect to the policy parameter θ. Doing gradient ascent $\theta = \theta + \nabla_\theta J$ therefore maximizes the expected discounted reward. Earlier work proposes the following policy gradient estimate to the objective J (Sutton & Barto, 2018):

$$g_{\text{policy},\theta} = \mathbb{E}_{\tau \sim \pi_\theta} \left[\sum_{t=0}^{T-1} \nabla_\theta \log \pi_\theta(a_t|s_t) G_t \right],$$

where $G_t = \sum_{k=0}^{\infty} \gamma^k r_{t+k}$ denotes the discounted return following time t. This gradient estimate, however, suffers from large variance (Sutton & Barto, 2018) and the following gradient estimate is suggested instead:

$$g_{\text{policy},\theta} = \mathbb{E}_{\tau} \left[\nabla_\theta \sum_{t=0}^{T-1} \log \pi_\theta(a_t|s_t) A(\tau, V, t) \right],$$

where $A(\tau, V, t)$ is the General Advantage Estimation (GAE) (Schulman et al., 2015), which measures "how good is a_t compared to the usual actions", and $V : S \rightarrow \mathbb{R}$ is the state-value function.

3 ACTION GUIDANCE

The key idea behind *action guidance* is to create a main agent that trains on the sparse rewards, and creating some auxiliary agents that are trained on shaped rewards. During the initial stages of training, the main agent has a high probability to take *action guidance* from the auxiliary agents, that is, the main agent can execute actions sampled from the auxiliary agents, rather than from its own policy. As the training goes on, this probability decreases, and the main agent executes more actions sampled from its own policy. During training, the main and auxiliary agents are updated via off-policy policy gradient. Our use of auxiliary agents makes the training sample-efficient, and our use of the main agent, who only sees its own sparse reward, makes sure that the agent will eventually optimize over the true objective of sparse rewards. In a way, *action guidance* can be seen as training agents using shaped rewards, while having the main agent learn by imitating from them.

Specifically, let us define $\mathcal{M}$ as the MDP that the main agent learns from and $\mathcal{A} = \{\mathcal{A}_1, \mathcal{A}_2, ..., \mathcal{A}_k\}$ be a set of auxiliary MDPs that the auxiliary agents learn from. In our constructions, $\mathcal{M}$ and $\mathcal{A}$ share the same state, observation, and action space. However, the reward function for $\mathcal{M}$ is $R_{\mathcal{M}}$, which is the sparse reward function, and reward functions for $\mathcal{A}$ are $R_{\mathcal{A}_1}, ..., R_{\mathcal{A}_k}$, which are the shaped reward functions. For each of these MDPs $\mathcal{E} \in \mathcal{S} = \{\mathcal{M}\} \cup \mathcal{A}$ above, let us initialize a policy $\pi_{\theta_\mathcal{E}}$ parameterized by parameters $\theta_\mathcal{E}$, respectively. Furthermore, let us use $\pi_\mathcal{S} = \{\pi_{\theta_\mathcal{E}} | \mathcal{E} \in \mathcal{S}\}$ to denote the set of these initialized policies.

At each timestep t, let us use some exploration strategy S that selects a policy $\pi_b \in \pi_\mathcal{S}$ to sample an action a_t given s_t. At the end of the episode, each policy $\pi_\theta \in \pi_\mathcal{S}$ can be updated via its off-policy policy gradient (Degris et al., 2012; Levine et al., 2020):

$$\mathbb{E}_{\tau \sim \pi_{\theta_b}} \left[\left(\prod_{t=0}^{T-1} \frac{\pi_\theta(a_t|s_t)}{\pi_{\theta_b}(a_t|s_t)} \right) \sum_{t=0}^{T-1} \nabla_\theta \log \pi_\theta(a_t|s_t) A(\tau, V, t) \right] \tag{1}$$

When $\pi_\theta = \pi_{\theta_b}$, the gradient in Equation 1 means on-policy policy gradient update for π_θ. Otherwise, the objective means off-policy policy gradient update for π_θ.

3.1 PRACTICAL ALGORITHM

The gradient in Equation 1 is unbiased, but its product of importance sampling ratio $\left(\prod_{t=0}^{T-1} \frac{\pi_\theta(a_t|s_t)}{\pi_{\theta_b}(a_t|s_t)} \right)$ is known to cause high variance (Wang et al., 2016). In practice, we clip the gradient the same way as Proximal Policy Gradient (PPO) (Schulman et al., 2017):

$$L^{CLIP}(\theta) = \mathbb{E}_{\tau \sim \pi_{\theta_b}} \left[\sum_{t=0}^{T-1} [\nabla_\theta \min(\rho_t(\theta) A(\tau, V, t), \text{clip}(\rho_t(\theta), \varepsilon) A(\tau, V, t))] \right] \tag{2}$$

$$\rho_t(\theta) = \frac{\pi_\theta(a_t|s_t)}{\pi_{\theta_b}(a_t|s_t)}, \quad \text{clip}(\rho_t(\theta), \varepsilon) = \begin{cases} 1 - \varepsilon & \text{if } \rho_t(\theta) < 1 - \varepsilon \\ 1 + \varepsilon & \text{if } \rho_t(\theta) > 1 + \varepsilon \\ \rho_t(\theta) & \text{otherwise} \end{cases}$$

During the optimization phase, the agent also learns the value function and maximize the policy's entropy. We therefore optimize the following joint objective for each $\pi_\theta \in \pi_S$:

$$L^{CLIP}(\theta) = L^{CLIP}(\theta) - c_1 L^{VF}(\theta) + c_2 S[\pi_{\theta_b}], \tag{3}$$

where c_1, c_2 are coefficients, S is an entropy bonus, and L^{VF} is the squared error loss for the value function associated with π_θ as done by Schulman et al. (2017). Although action guidance can be configured to leverage multiple auxiliary agents that learn diversified reward functions, we only use one auxiliary agent for the simplicity of experiments. In addition, we use ϵ-greedy as the exploration strategy S for determining the behavior policy. That is, at each timestep t, the behavior policy is selected to be $\pi_{\theta_\mathcal{M}}$ with probability $1 - \epsilon$ and $\pi_{\theta_\mathcal{D}}$ for $\mathcal{D} \in \mathcal{A}$ with probability ϵ (note that is ϵ is different from the clipping coefficient ε of PPO). Additionally, ϵ is set to be a constant 0.95 at start for some period of time steps (e.g. 800,000), which we refer to as the *shift* period (the time it takes to start "shifting" focus away from the auxiliary agents), then it is set to linearly decay to ϵ_{end} for some period of time steps (e.g. 1,000,000), which we refer to as the *adaptation* period (the time it takes for the main agent to fully "adapt" and become more independent).

3.2 POSITIVE LEARNING OPTIMIZATION

During our initial experiments, we found the main agent sometimes did not learn useful policies. Our hypothesis is that this was because the main agent is updated with too many trajectories with zero reward. Doing a large quantities of updates of these zero-reward trajectories actually causes the policy to converge prematurely, which is manifested by having low entropy in the action probability distribution.

To mitigate this issue of having too many zero-reward trajectories, we use a preliminary code-level optimization called Positive Learning Optimization (PLO). After collecting the rollouts, PLO works by skipping the gradient update for $\pi_{\theta_\mathcal{E}} \in \pi_S$ and its value function if the rollouts contains no reward according to $R_\mathcal{E}$. Intuitively, PLO makes sure that the main agent learns from meaningful experience that is associated with positive rewards. To confirm its effectiveness, we provide an ablation study of PLO in the experiment section.

4 EVALUATION

We use μRTS[3] as our testbed, which is a minimalistic RTS game maintaining the core features that make RTS games challenging from an AI point of view: simultaneous and durative actions, large branching factors and real-time decision making. To interface with μRTS, we use gym-microrts[4] (Huang & Ontañón, 2020) to conduct our experiments. The details of gym-microrts as a RL interface can be found at Appendix A.1.

4.1 TASKS DESCRIPTION

We examine the three following sparse reward tasks with a range of difficulties. For each task, we compare the performance of training agents with the sparse reward function $R_\mathcal{M}$, a shaped reward function $R_{\mathcal{A}_1}$, and action guidance with a single auxiliary agent learning from $R_{\mathcal{A}_1}$. Here are the descriptions of these environments and their reward functions.

1. LearnToAttack: In this task, the agent's objective is to learn move to the other side of the map where the enemy units live and start attacking them. Its $R_\mathcal{M}$ gives a +1 reward for each valid attack action the agent issues. This is of sparse reward because the action space is so large: the agent could have build a barracks or produce a unit; it is unlikely that the agents will by chance issue lots of moving actions (out of 6 action types) with correct directions (out of 4 directions) and then start attacking. Its $R_{\mathcal{A}_1}$ gives the difference between previous and current Euclidean distance between the enemy base and its closet unit owned by the agent as the shaped reward in addition to $R_\mathcal{M}$.

---

[3]`https://github.com/santiontanon/microrts`
[4]`https://github.com/vwxyzjn/gym-microrts`

2. ProduceCombatUnits: In this task, the agent's objective is to learn to build as many combat units as possible. Its $R_{\mathcal{M}}$ gives a +1 reward for each combat unit the agent produces. This is a more challenging task because the agent needs to learn 1) harvest resources, 2) produce barracks, 3) produce combat units once enough resources are gathered, 4) move produced combat units out of the way so as to not block the production of new combat units. Its $R_{\mathcal{A}_1}$ gives +1 for constructing every building (e.g. barracks), +1 for harvesting resources, +1 for returning resources, and +7 for each combat unit it produces.

3. DefeatRandomEnemy: In this task, the agent's objective is to defeat a biased random bot of which the attack, harvest and return actions have 5 times the probability of other actions. Additionally, the bot subjects to the same gym-microrts' limitation (See Appendix A.2) as the agents used in our experiments. Its $R_{\mathcal{M}}$ gives the match outcome as the reward (-1 on a loss, 0 on a draw and +1 on a win). This is the most difficult task we examined because the agent is subject to the full complexity of the game, being required to make both macro-decisions (e.g. deciding the high-level strategies to win the game) and micro-decisions (e.g. deciding which enemy units to attack. In comparison, its $R_{\mathcal{A}_1}$ gives +5 for winning, +1 for harvesting one resource, +1 for returning resources, +1 for producing one worker, +0.2 for constructing every building, +1 for each valid attack action it issues, +7 for each combat unit it produces, and $+(0.2 * d)$ where d is difference between previous and current Euclidean distance between the enemy base and its closet unit owned by the agent.

4.2 AGENT SETUP

We use PPO (Schulman et al., 2017) as the base DRL algorithm to incorporate action guidance. The details of the implementation, neural network architecture, hyperparameters, proper handling of μRTS's action space and invalid action masking (Huang & Ontañón, 2020) can be found in Appendix B. We compared the following strategies:

1. **Sparse reward (first baseline).** This agent is trained with PPO on $R_{\mathcal{M}}$ for each task.

2. **Shaped reward (second baseline).** This agent is trained with PPO on $R_{\mathcal{A}_1}$ for each task.

3. **Action guidance - long adaptation.** The agent is trained with PPO + action guidance with $shift = 2,000,000$ time steps, $adaptation = 7,000,000$ time steps, and $\epsilon_{end} = 0.0$

4. **Action guidance - short adaptation.** The agent is trained with PPO + action guidance with $shift = 800,000$ time steps, $adaptation = 1,000,000$ time steps, and $\epsilon_{end} = 0.0$

5. **Action guidance - mixed policy.** The agent is trained with PPO + action guidance with $shift = 2,000,000$ time steps and $adaptation = 2,000,000$ time steps, and $\epsilon_{end} = 0.5$. We call this agent "mixed policy" because it will eventually have 50% chance to sample actions from the main agent and 50% chance to sample actions from the auxiliary agent. It is effectively having mixed agent making decisions jointly.

Although it is desirable to add SAC-X to the list of strategies compared, it was not designed to handle domains with large discrete action spaces. Lastly, we also toggle the PLO option for action guidance - long adaptation, action guidance - short adaptation, action guidance - mixed policy, and sparse reward training strategies for a preliminary ablation study.

4.3 EXPERIMENTAL RESULTS

Each of the 6 strategies is evaluated in 3 tasks with 10 random seeds. We report the results in Table 1. All the learning curves can be found in Appendix C. Below are our observations.

Action guidance is almost as sample-efficient as reward shaping. Since the auxiliary agent learns from $R_{\mathcal{A}_1}$ and the main agent takes a lot of action guidance from the auxiliary agent during the shift period, the main agent is more likely to discover the first sparse reward more quickly and learn more efficiently. As an example, Figure 2 demonstrates such sample-efficiency in ProduceCombatUnits, where the agents trained with sparse reward struggle to obtain the very first reward. In comparison, most action guidance related agents are able to learn almost as fast as the agents trained with shaped reward.
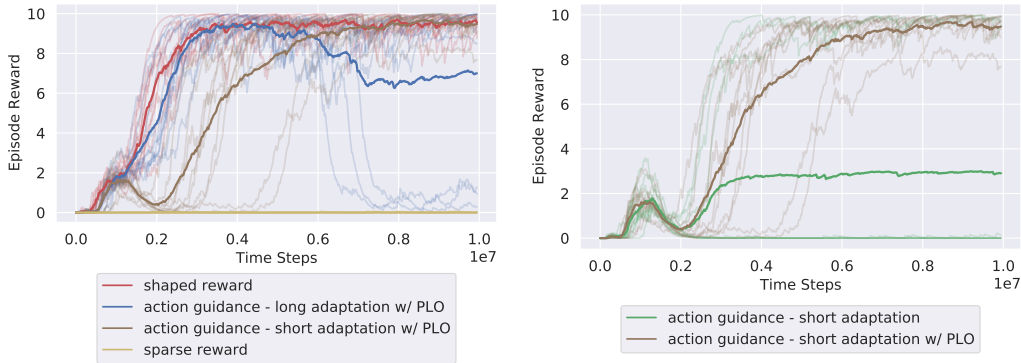
Figure 2: The faint lines are the actual episode reward of each seed for selected strategies in ProduceCombatUnits; solid lines are their means. The left figure showcase the sample-efficiency of action guidance; the right figure is a motivating example for PLO.

Table 1: The average episode reward (according to $R_\mathcal{M}$) achieved by each training strategy in each task over 10 random seeds.

	LearnToAttack	ProduceCombatUnit	DefeatRandomEnemy
sparse reward (first baseline)	3.30 ± 5.04	0.00 ± 0.01	-0.07 ± 0.03
sparse reward w/ PLO	0.00 ± 0.00	0.00 ± 0.01	-0.05 ± 0.03
shaped reward (second baseline)	10.00 ± 0.00	$\mathbf{9.57 \pm 0.30}$	0.08 ± 0.17
action guidance - long adaptation	$\mathbf{11.00 \pm 0.00}$	8.31 ± 2.62	0.11 ± 0.35
action guidance - long adaptation w/ PLO	$\mathbf{11.00 \pm 0.01}$	6.96 ± 4.04	$\mathbf{0.52 \pm 0.35}$
action guidance - mixed policy	$\mathbf{11.00 \pm 0.00}$	$\mathbf{9.67 \pm 0.17}$	0.40 ± 0.37
action guidance - mixed policy w/ PLO	10.67 ± 0.12	9.36 ± 0.35	0.30 ± 0.42
action guidance - short adaptation	$\mathbf{11.00 \pm 0.01}$	2.95 ± 4.48	-0.06 ± 0.04
action guidance - short adaptation w/ PLO	$\mathbf{11.00 \pm 0.00}$	9.48 ± 0.51	-0.05 ± 0.03

Action guidance eventually optimizes the sparse reward. This is perhaps the most important contribution of our paper. Action guidance eventually optimizes the main agent over the true objective, rather than optimizing shaped rewards. Using the ProduceCombatUnits task as an example, the agent trained with shaped reward would only start producing combat units once all the resources have been harvested, probably because the +1 reward for harvesting and returning resources are easy to retrieve and therefore the agents exploit them first. Only after these resources are exhausted would the agents start searching for other sources of rewards then learn producing combat units.

In contrast, the main agent of action guidance - short adaptation w/ PLO are initially guided by the shaped reward agent during the shift period. During the adaptation period, we find the main agent starts to optimize against the real objective by producing the first combat unit as soon as possible. This disrupts the behavior learned from the auxiliary agent and thus cause a visible degrade in the main agent's performance during 1M and 2M timesteps as shown in Figure 2. As the adaption period comes to an end, the main agent becomes fully independent and learn to produce combat units and harvest resources concurrently. This behavior matches the common pattern observed in professional RTS game players and is obviously more desirable because should the enemy attack early, the agent will have enough combat units to defend.

In the DefeatRandomEnemy task, the agents trained with shaped rewards learn a variety of behaviors; some of them learn to do a worker rush while others learn to focus heavily on harvesting resources and producing units. This is likely because the agents could get similar level of shaped rewards despite having diverse set of behaviors. In comparison, the main agent of action guidance - long adaptation w/ PLO would start optimizing the sparse reward after the shift period ends; it almost always learns to do a worker rush, which an efficient way to win against a random enemy as shown in Figure 1.

The hyper-parameters adaptation and shift matter. Although the agents trained with action guidance - short adaptation w/ PLO learns the more desirable behavior, they perform considerably worse

7

(a) shaped reward
(https://streamable.com/ytpt7u)
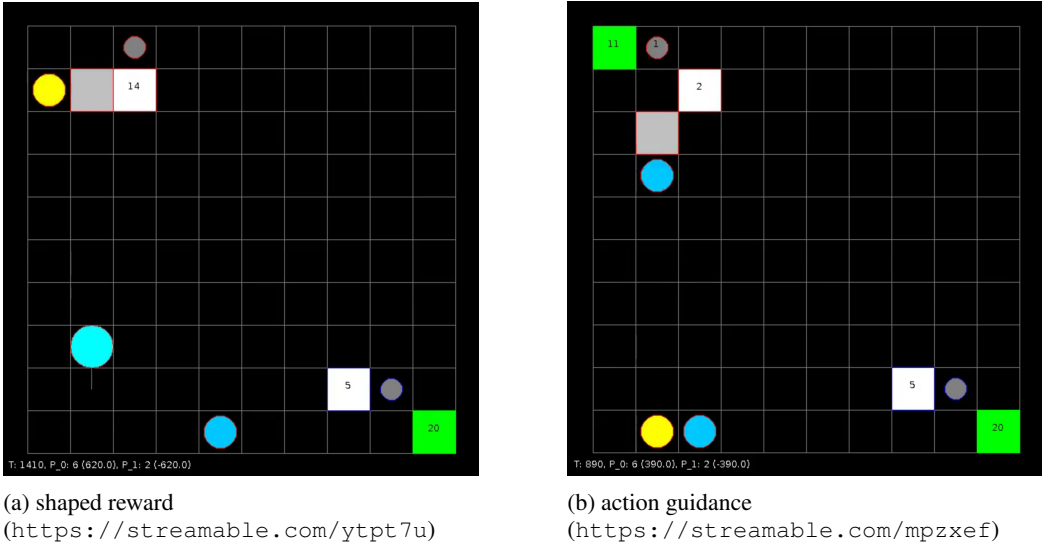
(b) action guidance
(https://streamable.com/mpzxef)

Figure 3: The screenshot shows the typical learned behavior of agents in the task of ProduceCombatUnits. (a) shows an agent trained with shaped reward function $R_{\mathcal{A}_1}$ learn to only produce combat units once the resources are exhausted (i.e. it produces three combat units at $t = 1410$). In contrary, (b) shows an agent trained with action guidance learn to produce units and harvest resources concurrently (i.e. it produces three combat units at $t = 890$). Click on the link below figures to see the full videos of trained agents.

in the harder task of DefeatRandomEnemy. It suggests the harder that task is perhaps the longer adaptation should be set. However, in ProduceCombatUnits, agents trained with action guidance - long adaptation w/ PLO exhibits the same category of behavior as agents trained with shaped reward, where the agent would only start producing combat units once all the resources have been harvested. A reasonable explanation is that higher adaptation gives more guidance to the main agents to consistently find the sparse reward, but it also inflicts more bias on how the task should be accomplished; lower adaption gives less guidance but increase the likelihood for the main agents to find better ways to optimize the sparse rewards.

Positive Learning Optimization results are inconclusive. We found PLO to be an interesting yet sometimes effective optimization in stabilizing the performance for agents trained with action guidance. As a motivating example, Figure 2 showcases the actual episode reward of 10 seeds in ProduceCombatUnits, where agents trained with action guidance - short adaptation and PLO seem to always converge while agents trained without PLO would only sometimes converge. However, PLO does not always help. For example, PLO actually hurt the performance of action guidance - long adaptation in ProduceCombatUnits by having a few degenerate runs as shown in Figure 2. It is also worth noting the PLO does not help the sparse reward agent at all, suggesting PLO is a an optimization somewhat unique to action guidance.

Action guidance - mixed policy is viable. According to Table 1, agents trained with action guidance - mixed policy with or without PLO seem to perform relatively well in all three tasks examined. This is a interesting discovery because it suggests action guidance could go both ways: the auxiliary agents could also benefit from the learned policies of the main agent. An alternative perspective is to consider the main agent and the auxiliary agents as a whole entity that mixes different reward functions, somehow making joint decision and collaborating to accomplish common goals.

5   CONCLUSIONS

In this paper, we present a novel technique called *action guidance* that successfully trains the agent to eventually optimize over sparse rewards yet does not lose the sample efficiency that comes with reward shaping, effectively getting the best of both worlds. Our experiments with DefeatRandomEnemy in particular show it is possible to train a main agent on the full game of μRTS using only the

match outcome reward, which suggests action guidance could serve as a promising alternative to the training paradigm of AlphaStar (Vinyals et al., 2019) that uses supervised learning with human replay data to bootstrap an agent. As part of our future work, we would like to scale up the approach to defeat stronger opponents.

REFERENCES

Pieter Abbeel and Andrew Y Ng. Apprenticeship learning via inverse reinforcement learning. In *Proceedings of the twenty-first international conference on Machine learning*, pp. 1, 2004.

Marcin Andrychowicz, Filip Wolski, Alex Ray, Jonas Schneider, Rachel Fong, Peter Welinder, Bob McGrew, Josh Tobin, OpenAI Pieter Abbeel, and Wojciech Zaremba. Hindsight experience replay. In *Advances in neural information processing systems*, pp. 5048–5058, 2017.

Michael Bain and Claude Sammut. A framework for behavioural cloning. In *Machine Intelligence 15*, pp. 103–129, 1995.

Marc Bellemare, Sriram Srinivasan, Georg Ostrovski, Tom Schaul, David Saxton, and Remi Munos. Unifying count-based exploration and intrinsic motivation. In *Advances in neural information processing systems*, pp. 1471–1479, 2016.

Christopher Berner, Greg Brockman, Brooke Chan, Vicki Cheung, Przemyslaw Debiak, Christy Dennison, David Farhi, Quirin Fischer, Shariq Hashme, Chris Hesse, Rafal Józefowicz, Scott Gray, Catherine Olsson, Jakub W. Pachocki, Michael Petrov, Henrique Pond'e de Oliveira Pinto, Jonathan Raiman, Tim Salimans, Jeremy Schlatter, Jonas Schneider, Szymon Sidor, Ilya Sutskever, Jie Tang, Filip Wolski, and Susan Zhang. Dota 2 with large scale deep reinforcement learning. *ArXiv*, abs/1912.06680, 2019.

Greg Brockman, Vicki Cheung, Ludwig Pettersson, Jonas Schneider, John Schulman, Jie Tang, and Wojciech Zaremba. Openai gym. *arXiv preprint arXiv:1606.01540*, 2016.

Yuri Burda, Harri Edwards, Deepak Pathak, Amos Storkey, Trevor Darrell, and Alexei A. Efros. Large-scale study of curiosity-driven learning. In *ICLR*, 2019.

Thomas Degris, Martha White, and Richard S Sutton. Off-policy actor-critic. *arXiv preprint arXiv:1205.4839*, 2012.

Prafulla Dhariwal, Christopher Hesse, Oleg Klimov, Alex Nichol, Matthias Plappert, Alec Radford, John Schulman, Szymon Sidor, Yuhuai Wu, and Peter Zhokhov. Openai baselines. `https://github.com/openai/baselines`, 2017.

Thomas G Dietterich. Hierarchical reinforcement learning with the maxq value function decomposition. *Journal of artificial intelligence research*, 13:227–303, 2000.

Logan Engstrom, Andrew Ilyas, Shibani Santurkar, Dimitris Tsipras, Firdaus Janoos, Larry Rudolph, and Aleksander Madry. Implementation matters in deep rl: A case study on ppo and trpo. In *International Conference on Learning Representations*, 2019.

Rein Houthooft, Xi Chen, Yan Duan, John Schulman, Filip De Turck, and Pieter Abbeel. Curiosity-driven exploration in deep reinforcement learning via bayesian neural networks. 2016.

Shengyi Huang and Santiago Ontañón. A closer look at invalid action masking in policy gradient algorithms. *arXiv preprint arXiv:2006.14171*, 2020.

Shengyi Huang and Santiago Ontañón. Comparing observation and action representations for deep reinforcement learning in μrts. 2019.

Anssi Kanervisto, Christian Scheller, and Ville Hautamäki. Action space shaping in deep reinforcement learning. *arXiv preprint arXiv:2004.00980*, 2020.

Diederik P Kingma and Jimmy Ba. Adam: A method for stochastic optimization. *arXiv preprint arXiv:1412.6980*, 2014.

Sergey Levine, Aviral Kumar, George Tucker, and Justin Fu. Offline reinforcement learning: Tutorial, review, and perspectives on open problems. *arXiv preprint arXiv:2005.01643*, 2020.

Manuel Lopes, Tobias Lang, Marc Toussaint, and Pierre-Yves Oudeyer. Exploration in model-based reinforcement learning by empirically estimating learning progress. In *Advances in neural information processing systems*, pp. 206–214, 2012.

Vinod Nair and Geoffrey E Hinton. Rectified linear units improve restricted boltzmann machines. In *Proceedings of the 27th international conference on machine learning (ICML-10)*, pp. 807–814, 2010.

Sanmit Narvekar and Peter Stone. Learning curriculum policies for reinforcement learning. *arXiv preprint arXiv:1812.00285*, 2018.

Andrew Y Ng, Daishi Harada, and Stuart Russell. Policy invariance under reward transformations: Theory and application to reward shaping. 1999.

Zhen-Jia Pang, Ruo-Ze Liu, Zhou-Yu Meng, Yi Zhang, Yang Yu, and Tong Lu. On reinforcement learning for full-length game of starcraft. In *Proceedings of the AAAI Conference on Artificial Intelligence*, volume 33, pp. 4691–4698, 2019.

Deepak Pathak, Pulkit Agrawal, Alexei A. Efros, and Trevor Darrell. Curiosity-driven exploration by self-supervised prediction. In *ICML*, 2017.

Martin Riedmiller, Roland Hafner, Thomas Lampe, Michael Neunert, Jonas Degrave, Tom Van de Wiele, Volodymyr Mnih, Nicolas Heess, and Jost Tobias Springenberg. Learning by playing-solving sparse reward tasks from scratch. *arXiv preprint arXiv:1802.10567*, 2018.

Tom Schaul, Daniel Horgan, Karol Gregor, and David Silver. Universal value function approximators. In *International conference on machine learning*, pp. 1312–1320, 2015.

John Schulman, Philipp Moritz, Sergey Levine, Michael Jordan, and Pieter Abbeel. High-dimensional continuous control using generalized advantage estimation. *arXiv preprint arXiv:1506.02438*, 2015.

John Schulman, Filip Wolski, Prafulla Dhariwal, Alec Radford, and Oleg Klimov. Proximal policy optimization algorithms. *arXiv preprint arXiv:1707.06347*, 2017.

Richard S Sutton and Andrew G Barto. *Reinforcement learning: An introduction*. MIT press, 2018.

Maxwell Svetlik, Matteo Leonetti, Jivko Sinapov, Rishi Shah, Nick Walker, and Peter Stone. Automatic curriculum graph generation for reinforcement learning agents. In *Thirty-First AAAI Conference on Artificial Intelligence*, 2017.

Matthew E. Taylor, Peter Stone, and Yaxin Liu. Transfer learning via inter-task mappings for temporal difference learning. *J. Mach. Learn. Res.*, 8:2125–2167, 2007.

Oriol Vinyals, Timo Ewalds, Sergey Bartunov, Petko Georgiev, Alexander Sasha Vezhnevets, Michelle Yeo, Alireza Makhzani, Heinrich Küttler, John Agapiou, Julian Schrittwieser, et al. Starcraft ii: A new challenge for reinforcement learning. *arXiv preprint arXiv:1708.04782*, 2017.

Oriol Vinyals, Igor Babuschkin, Wojciech M Czarnecki, Michaël Mathieu, Andrew Dudzik, Junyoung Chung, David H Choi, Richard Powell, Timo Ewalds, Petko Georgiev, et al. Grandmaster level in starcraft ii using multi-agent reinforcement learning. *Nature*, 575(7782):350–354, 2019.

Ziyu Wang, Victor Bapst, Nicolas Heess, Volodymyr Mnih, Remi Munos, Koray Kavukcuoglu, and Nando de Freitas. Sample efficient actor-critic with experience replay. *arXiv preprint arXiv:1611.01224*, 2016.

Deheng Ye, Zhao Liu, Mingfei Sun, Bei Shi, Peilin Zhao, Hao Wu, Hongsheng Yu, Shaojie Yang, Xipeng Wu, Qingwei Guo, et al. Mastering complex control in moba games with deep reinforcement learning. In *AAAI*, pp. 6672–6679, 2020.

APPENDICES

A   DETAILS ON μRTS AS A REINFORCEMENT LEARNING ENVIRONMENT

For all of our experiments in this paper, we use the *gym-microrts* (Huang & Ontañón, 2019) library which provides a reinforcement learning interface of μRTS similar to OpenAI Gym's interface (Brockman et al., 2016). In this section, we hope to provide details on the implementation of *gym-microrts* as well as its limitations.

A.1   OBSERVATION AND ACTION SPACE OF μRTS

Here is a description of *gym-microrts*'s observation and action space:

- **Observation Space.** Given a map of size $h \times w$, the observation is a tensor of shape (h, w, n_f), where n_f is a number of feature planes that have binary values. The observation space used in this paper uses 27 feature planes as shown in Table 2. A feature plane can be thought of as a concatenation of multiple one-hot encoded features. As an example, if there is a worker with hit points equal to 1, not carrying any resources, owner being Player 1, and currently not executing any actions, then the one-hot encoding features will look like the following:

$$[0, 1, 0, 0, 0], [1, 0, 0, 0, 0], [1, 0, 0],$$
$$[0, 0, 0, 0, 1, 0, 0, 0], [1, 0, 0, 0, 0, 0]$$

  The 27 values of each feature plane for the position in the map of such worker will thus be:

$$[0, 1, 0, 0, 0, 1, 0, 0, 0, 0, 1, 0, 0, 0, 0, 0, 0, 1, 0, 0, 0, 1, 0, 0, 0, 0, 0]$$

- **Action Space.** Given a map of size $h \times w$, the action is an 8-dimensional vector of discrete values as specified in Table 2. The first component of the action vector represents the unit in the map to issue actions to, the second is the action type, and the rest of components represent the different parameters different action types can take.

A.2   LIMITATIONS

In general, there are two limitations associated with *gym-microrts*'s reinforcement learning interface that could hinder the trained agents from competing against existing μRTS bots. As a result, the agent trained in this paper would subject to these limitations.

Frame-skipping   Each action in μRTS takes some internal game time, measured in ticks, for the action to be completed. *gym-microrts* sets the time of performing harvest action, return action, and move action to be 10 game ticks. Once an action is issued to a particular unit, the unit would be considered as a "busy" unit and would take additional 9 game ticks for the actions to be finalized. To speed up training, *gym-microrts* by default performs frame skipping of 9 frames such that from the agent's perspective, once it executes the harvest action, return action, or move action given the current observation, those actions would be finished in the next observation.

Limited Unit Action per Tick   In general, the game engine of μRTS allows the bots to issue actions to as many units as the bots own at each game tick. This means the action space will have "varied size" depending on the number of units available for control. For simplicity, *gym-microrts* only allows the agent to issue one action to one unit at each tick.

B   DETAILS ON THE TRAINING ALGORITHM PROXIMAL POLICY OPTIMIZATION

The DRL algorithm that we use to train the agent is Proximal Policy Optimization (PPO) Schulman et al. (2017), one of the state of the art algorithms available. The hyper-parameters of our experiments can be found in Table 3. There are three important details regarding our PPO implementation that warrants explanation. The first detail concerns how to generate an action in the `MultiDiscrete` action space as defined in the OpenAI Gym environment (Brockman et al., 2016) of gym-microrts (Huang & Ontañón, 2019), the second details involves the implementation of invalid action masking (Vinyals et al., 2017; Berner et al., 2019; Huang & Ontañón, 2020) with PPO, and the third detail is about the various code-level optimizations utilized to augment performance. As pointed out by Engstrom, Ilyas, et al. (Engstrom et al., 2019), such code-level optimizations could be critical to the performance of PPO.

Table 2: The descriptions of observation features and action components.

Observation Features	Planes	Description
Hit Points	5	$0, 1, 2, 3, \geq 4$
Resources	5	$0, 1, 2, 3, \geq 4$
Owner	3	player 1, -, player 2
Unit Types	8	-, resource, base, barrack, worker, light, heavy, ranged
Current Action	6	-, move, harvest, return, produce, attack

Action Components	Range	Description
Source Unit	$[0, h \times w - 1]$	the location of unit selected to perform an action
Action Type	$[0, 5]$	NOOP, move, harvest, return, produce, attack
Move Parameter	$[0, 3]$	north, east, south, west
Harvest Parameter	$[0, 3]$	north, east, south, west
Return Parameter	$[0, 3]$	north, east, south, west
Produce Direction Parameter	$[0, 3]$	north, east, south, west
Produce Type Parameter	$[0, 5]$	resource, base, barrack, worker, light, heavy, ranged
Attack Target Unit	$[0, h \times w - 1]$	the location of unit that will be attacked

B.1 Multi Discrete Action Generation

To perform an action a_t in μRTS, according to Table 2, we have to select a Source Unit, Action Type, and its corresponding action parameters. So in total, there are $hw \times 6 \times 4 \times 4 \times 4 \times 4 \times 6 \times hw = 9216(hw)^2$ number of possible discrete actions (including invalid ones), which grows exponentially as we increase the map size. If we apply the PPO directly to this discrete action space, it would be computationally expensive to generate the distribution for $9216(hw)^2$ possible actions. To simplify this combinatorial action space, `openai/baselines` Dhariwal et al. (2017) library proposes an idea to consider this discrete action to be composed from some smaller *independent* discrete actions. Namely, a_t is composed of smaller actions

$$a_t^{\text{Source Unit}}, a_t^{\text{Action Type}}, a_t^{\text{Move Parameter}}, a_t^{\text{Harvest Parameter}},$$
$$a_t^{\text{Return Parameter}}, a_t^{\text{Produce Direction Parameter}}, a_t^{\text{Produce Type Parameter}}, a_t^{\text{Attack Target Unit}}$$

And the policy gradient is updated in the following way (without considering the PPO's clipping for simplicity)

$$\sum_{t=0}^{T-1} \nabla_\theta \log \pi_\theta(a_t|s_t) G_t = \sum_{t=0}^{T-1} \nabla_\theta \left(\sum_{d \in D} \log \pi_\theta(a_t^d|s_t) \right) G_t$$
$$= \sum_{t=0}^{T-1} \nabla_\theta \log \left(\prod_{d \in D} \pi_\theta(a_t^d|s_t) \right) G_t$$

$D = \{$Source Unit, Action Type, Move Parameter, Harvest Parameter, Return Parameter, Produce Direction Parameter, Produce Type Parameter, Attack Target Unit, $\}$

Implementation wise, for each Action Component of range $[0, x-1]$, the logits of the corresponding shape x is generated, which we call Action Component logits, and each a_t^d is sampled from this Action Component logits. Because of this idea, the algorithm now only has to generate $hw + 6 + 4 + 4 + 4 + 4 + 6 + hw = 2hw + 36$ number of logits, which is significantly less than $9216(hw)^2$. To the best of our knowledge, this approach of handling large multi discrete action space is only mentioned by Kanervisto et, al Kanervisto et al. (2020).

B.2 Invalid Action Masking

Invalid action masking is a technique that "masks out" invalid actions and then just sample from those actions that are valid (Vinyals et al., 2017; Berner et al., 2019). Huang & Ontañón (2020) show invalid action masking is crucial in helping the agents explore in μRTS

Table 3: The list of hyperparameters and their values.

Parameter Names	Parameter Values
Total Time Steps	1,000,000
Number of Mini-batches	4
Number of Environments	8
Number of Steps per Environment	128
γ (Discount Factor)	0.99
λ (for GAE)	0.95
ε (PPO's Clipping Coefficient)	0.1
η (Entropy Regularization Coefficient)	0.01
ω (Gradient Norm Threshold)	0.5
K (Number of PPO Update Iteration Per Epoch)	4
α Learning Rate	0.00025 Linearly Decreased to 0 over the Total Time Steps
$c1$ (Value Function Coefficient, see Equation 3)	0.5
$c2$ (Entropy Coefficient, see Equation 3)	0.01

B.3 CODE-LEVEL OPTIMIZATIONS

Here is a list of code-level optimizations utilized in this experiments. For each of these optimizations, we include a footnote directing the readers to the files in the *openai/baselines* (Dhariwal et al., 2017) that implements these optimization.

1. **Normalization of Advantages**[5]**:** After calculating the advantages based on GAE, the advantages vector is normalized by subtracting its mean and divided by its standard deviation.

2. **Normalization of Observation**[6]**:** The observation is pre-processed before feeding to the PPO agent. The raw observation was normalized by subtracting its running mean and divided by its variance; then the raw observation is clipped to a range, usually $[-10, 10]$.

3. **Rewards Scaling**[7]**:** Similarly, the reward is pre-processed by dividing the running variance of the discounted the returns, following by clipping it to a range, usually $[-10, 10]$.

4. **Value Function Loss Clipping**[8]**:** The PPO implementation of *openai/baselines* clips the value function loss in a manner that is similar to the PPO's clipped surrogate objective:

$$V_{loss} = \max\left[\left(V_{\theta_t} - V_{targ}\right)^2, \left(V_{\theta_{t-1}} + \text{clip}\left(V_{\theta_t} - V_{\theta_{t-1}}, -\varepsilon, \varepsilon\right)\right)^2\right]$$

where V_{targ} is calculated by adding $V_{\theta_{t-1}}$ and the A calculated by General Advantage EstimationSchulman et al. (2015).

5. **Adam Learning Rate Annealing**[9]**:** The Adam Kingma & Ba (2014) optimizer's learning rate is set to decay as the number of timesteps agent trained increase.

6. **Mini-batch updates**[10]**:** The PPO implementation of the *openai/baselines* also uses mini-batches to compute the gradient and update the policy instead of the whole batch data such as in *open/spinningup*. The mini-batch sampling scheme, however, still makes sure that

---

[5]https://github.com/openai/baselines/blob/ea25b9e8b234e6ee1bca43083f8f3cf974143998/baselines/ppo2/model.py#L139
[6]https://github.com/openai/baselines/blob/ea25b9e8b234e6ee1bca43083f8f3cf974143998/baselines/common/vec_env/vec_normalize.py#L4
[7]https://github.com/openai/baselines/blob/ea25b9e8b234e6ee1bca43083f8f3cf974143998/baselines/common/vec_env/vec_normalize.py#L4
[8]https://github.com/openai/baselines/blob/ea25b9e8b234e6ee1bca43083f8f3cf974143998/baselines/ppo2/model.py#L68-L75
[9]https://github.com/openai/baselines/blob/ea25b9e8b234e6ee1bca43083f8f3cf974143998/baselines/ppo2/ppo2.py#L135
[10]https://github.com/openai/baselines/blob/ea25b9e8b234e6ee1bca43083f8f3cf974143998/baselines/ppo2/ppo2.py#L160-L162
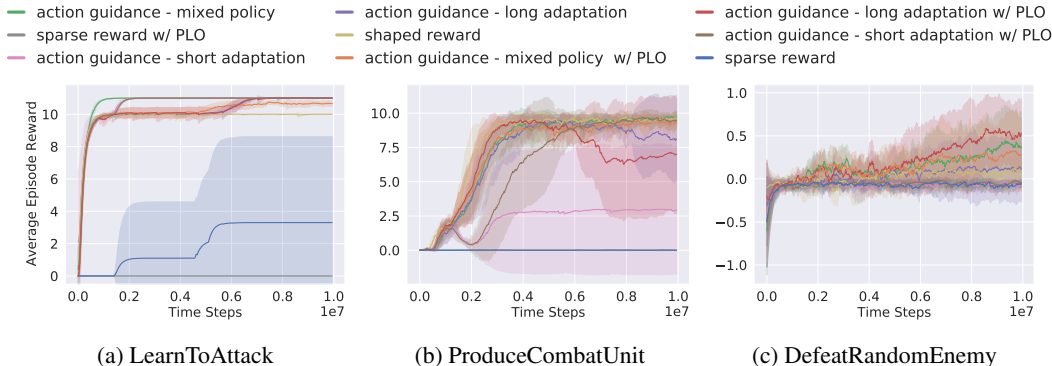
Figure 4: The learning curves of agents. The x-axis shows the number of time steps and y-axis shows the average episode reward gathered.

every transition is sampled only once, and that the all the transitions sampled are actually for the network update.

7. **Global Gradient Clipping**[11]**:** For each update iteration in an epoch, the gradients of the policy and value network are clipped so that the "global ℓ_2 norm" (i.e. the norm of the concatenated gradients of all parameters) does not exceed 0.5.

8. **Orthogonal Initialization of weights**[12]**:** The weights and biases of fully connected layers use with orthogonal initialization scheme with different scaling. For our experiments, however, we always use the scaling of 1 for historical reasons.

B.4   NEURAL NETWORK ARCHITECTURE

The input to the neural network is a tensor of shape $(10, 10, 27)$. The first hidden layer convolves 16 3×3 filters with stride 2 with the input tensor followed by a rectifier nonlinearityNair & Hinton (2010). The second hidden layer similarly convolves 32 2×2 filters followed by a rectifier nonlinearity. The final hidden layer is a fully connected linear layer consisting of 128 rectifier units. The policy's output layer is a fully connected linear layer with $2hw + 36 = 236$ number of output and the value output layer is a fully connected linear layer with a single output.

C   LEARNING CURVES

The learning curves of all experiments are shown in Figure 4.

---

[11]https://github.com/openai/baselines/blob/ea25b9e8b234e6ee1bca43083f8f3cf974143998/baselines/ppo2/model.py#L107
[12]https://github.com/openai/baselines/blob/ea25b9e8b234e6ee1bca43083f8f3cf974143998/baselines/a2c/utils.py#L58